Inhibitory effect of fungoid chitosan in the generation of aldehydes relevant to photooxidative decay in a sulphite-free white wine

Antonio Castro Marin, Pierre Stocker, Fabio Chinnici, Mathieu Cassien, Sophie Thétiot-Laurent, Nicolas Vidal, Claudio Riponi, Bertrand Robillard, Marcel Culcasi, Sylvia Pietri

HAL Id: hal-03018950

https://amu.hal.science/hal-03018950

Submitted on 23 Nov 2020

1 **Inhibitory effect of fungoid chitosan in the generation of aldehydes**

2 **relevant to photooxidative decay in a sulphite-free white wine**

3

4 Antonio Castro Marin[a,b], Pierre Stocker[a], Fabio Chinnici[b], Mathieu Cassien[a,c],

5 Sophie Thétiot-Laurent[a], Claudio Riponi[b], Bertrand Robillard[d], Marcel Culcasi[a]*

6 and Sylvia Pietri[a]

7

8 Addresses:

9 [a]Aix Marseille Univ, CNRS, ICR, Marseille, France.

10 [b]Department of Agricultural and Food Sciences, University of Bologna, Bologna, Italy.

11 [c]Yelen Analytics, Ensuès-la-Redonne, France.

12 [d]Institut Œnologique de Champagne, Epernay, France.

13

14 Corresponding author: Marcel Culcasi, PhD

15 Institut de Chimie Radicalaire, Sondes Moléculaires en Biologie et Stress Oxydant,

16 Aix Marseille Université, CNRS UMR 7273

17 Centre Scientifique de Saint-Jérôme, Avenue Escadrille Normandie Niemen, Service 522

18 13397 Marseille cedex 13, France

19 Tel: 00 33 (0)4 91 28 90 25

20 email: marcel.culcasi@univ-amu.fr

21

22

Abstract

The reaction pathways were investigated by which a fungoid chitosan (CsG) may protect against photooxidative decay of model solutions and a sulphite-free white wine. Samples containing CsG were dark incubated for 2 days before exposure to fluorescent lighting for up to 21 days in the presence of wine like (+)-catechin and/or iron doses. In both systems CsG at winemaking doses significantly reduced the photoproduction of acetaldehyde and, to a better extent, glyoxylic acid, two key reactive aldehydes implicated in wine oxidative spoilage. After 21 days, CsG was two-fold more effective than sulphur dioxide in preventing glyoxylic acid formation and minimizing the browning of white wine. Among the antioxidant mechanisms involved in CsG protective effect, iron chelation, and hydrogen peroxide quenching were demonstrated. Besides, the previously unreported tartrate displacement from the [iron(III)-tartrate] complex was revealed as an additional inhibitory mechanism of CsG under photo-Fenton oxidation conditions.

Highlights

1. Fungoid chitosan reduces the generation of aldehydes during wine photooxidation
2. Chitosan reduces iron amounts in solution by adsorbing [carboxylates-Fe(III)] complexes
3. In extended oxidative conditions SO_2 is a poorer wine anti-browning agent than chitosan
4. Sulphites better control free acetaldehyde but not glyoxylic acid amounts
5. In wines chitosan can mitigate the browning while preserving catechin amounts

Abbreviations: ANOVA, analysis of variance; CsG, chitosan.

1. Introduction

The optimal management of wine oxidation represents a huge challenge for winemakers. From a sensory point of view, controlled oxidation could be beneficial for red wines due to the reduction of astringency and the enhancement of colour stabilization. However, white wines are usually damaged by air exposure which can lead to unwanted non-enzymatic browning, and the decay of both the sensory characteristics (aromatic defects, increase of astringency), and nutritional properties (Waterhouse & Laurie, 2006).

In oenology, oxidation involves enzymatic or non-enzymatic reactions. However, after the inactivation of must polyphenol oxidases during the alcoholic fermentation, non-enzymatic cascade becomes the main oxidative pathway throughout the winemaking process commonly carried out in wineries, and it remains still active upon bottling and at storage. During wine oxidation, a sequence of univalent reduction steps settles from oxygen up to water, via a Fe(II)/Fe(III) redox cycle where hydrogen peroxide (H_2O_2), and the highly reactive hydroxyl radical (HO•) are formed (Waterhouse & Laurie, 2006; Oliveira, Ferreira, De Freitas, & Silva, 2011; Danilewicz, 2012). The most conclusive proof of HO• formation in wine oxidation came from electron paramagnetic resonance (EPR) studies (Elias, Andersen, Skibsted, & Waterhouse, 2009; Nikolantonaki et al., 2019; Castro Marín et al., 2019; Marchante et al., 2020) showing that 1-hydroxyethyl radical (1-HER) is transiently generated during the conversion of ethanol into acetaldehyde, a reaction forming H_2O_2 (Fig. 1).

The reduction of H_2O_2 to HO• is mediated by metal ions (e.g., by the Fe(II)/Fe(III) redox couple) according to the so-called 'thermal' (as opposed to light-induced) Fenton mechanism (black pathway in Fig. 1). In this process wine polyphenols play a major role

73 by redox cycling iron (Oliveira et al., 2011; Danilewicz, 2012). Fenton-derived HO• will also

74 react with wine carboxylic acids such as tartaric acid (a major component in grape juice),

75 forming a carbon-centered radical derivative which undergoes oxidation and

76 decarboxylation steps to yield glyoxylic acid. Hence, acetaldehyde and glyoxylic acid are

77 main intermediates in the oxidative evolution of wine (Drinkine, Glories, & Saucier, 2005).

78 These compounds have been shown to cross-link wine flavan-3-ols to yield methyne-

79 bridged dimers, which in turn decompose into (*i*) 8-vinylflavan-3-ols adducts (Fulcrand,

80 Dueñas, Salas, & Cheynier, 2006) in the case of acetaldehyde, and (*ii*) yellow-brown

81 xanthylium cation pigments that contribute to the chemical browning of white wines (Es-

82 Safi et al., 1999; Bührle, Gohl, & Weber, 2017), in the case of glyoxylic acid. Figure 1

83 stresses on 8-vinyl-(+)-catechin, the unstable acetaldehyde adduct formed when (+)-

84 catechin is the flavan-3-ol substrate, as this class of compounds brings about browning

85 upon condensing with anthocyanins (Mateus et al., 2002; Cruz et al., 2009) and/or reacting

86 with quinones through electron transfer reactions (Cruz et al., 2009).

87   Accordingly, reducing the development of aldehydic oxidation intermediates would be

88 a relevant strategy to limit browning spoilage of wines. Possessing antimicrobial

89 properties, sulphur dioxide (SO_2) is widely used in oenology for its global antioxidant

90 power, acting upstream (by scavenging H_2O_2 and reducing quinones back to their phenolic

91 precursors) or downstream (by binding acetaldehyde) to HO• formation (Danilewicz, 2007;

92 Oliveira et al., 2011). However, an increasing number of consumers are turning toward

93 non-sulphited wines because sulphites have been associated with many adverse health

94 effects, (Vally, Misso, & Madan, 2009).

95   Another strategy not involving SO_2 to preserve shelf life of finished wines and to

96 prevent chemical browning would be inhibiting specifically free radical processes shown in

97 Figure 1. This has promoted the use of antioxidant additives such as glutathione or

98 ascorbic acid (Sonni, Clark, Prenzler, Riponi et al., 2011a; Barril, Clark, & Scollary, 2012;

Marchante et al., 2020). Alternatively, use of metal chelators to prevent the Fenton reaction is gaining popularity. Among the few biocompatible, biodegradable and non-toxic potential candidates chitosan, the deacetylated derivative of chitin found in the carapace of shellfish, insects, green algae or fungi, is of great interest in food science, having versatile functionalities as antimicrobial and bacteriostatic, and able to form a variety of films, hydrogels or nanoparticles (Qin et al., 2002; Muxika, Etxabide, Uranga, Guerrero, et al., 2017).

Owing to its metal chelation power, chitosan from fungal origin has been recommended in 2009 by the International Organisation of Vine and Wine (OIV), then authorized by the EU as an additive in winemaking for removing metals and pollutants, preventing cloudiness, and for the reduction of *Brettanomyces* spp and other undesirable wine microbial population (EC Regulation No 53/2011). As a consequence, previous studies in real wines or model solutions have focused on the efficacy of chitosan in reducing the tendency to browning (Spagna et al., 1996) and diminishing the oxidative degradation of one of its chemical determinants, (+)-catechin (Fig. 1) (Chinnici, Natali, & Riponi, 2014), with no or little impact on polyphenols content and fermentative aromatic compounds (Filipe-Ribeiro, Cosme & Nunes, 2018; Colangelo, Torchio, De Faveri, & Lambri, 2018; Picariello, Rinaldi, Blaiotta, Moio, Pirozzi, & Gambuti, 2020). In a recent EPR work (Castro Marín et al., 2019), a chronology of the antioxidant protection afforded by dark pretreatment (2 days) with chitosan of a SO_2-free white wine was proposed, first involving partial inactivation of the wine catalytic iron pool by complexation, followed by direct scavenging of HO• formed by thermal Fenton reaction catalyzed by those iron ions having escaped chelation. In connection with chemical browning, the same authors (Castro Marín et al., 2019) observed a significant inhibition of acetaldehyde formation when oxidation of the wine was provoked by UV-Vis illumination.

In view of the above, the aim of this study was to decipher some mechanisms implicated in this latter effect of chitosan on acetaldehyde photoproduction. Indeed, storing bottled white wines under UV-Vis light for long periods is known to accelerate oxidation, affecting the main oenological attributes and leading to browning. A first mechanism of photooxidation involves the photochemical cleavage of iron(III) aquacomplex $Fe(H_2O)_5(OH)^{2+}$ (abbreviated as $Fe(OH)^{2+}$), the major form of aqueous ferric ions at wine pH, to generate HO• in a process termed as 'photo-Fenton' (green pathway in Fig. 1) (Loures et al., 2013). Another wine relevant pathway has been demonstrated, whereby photolysis of the [iron(III)-tartrate] complex, the predominant form of Fe(III) found in wine, regenerates ferrous ions and a transient tartaric acid derived acyloxyl radical, which subsequently decomposes into glyoxylic acid by a sequence of oxidation/decarboxylation reactions (red pathway in Fig. 1) that ultimately provoke browning (Grant-Preece, Schmidtke, Barril, & Clark, 2017a, b).

In real white wine samples spiked with a relevant Fe(II) concentration and added allowed doses of chitosan or SO_2, there was a similar inhibition of acetaldehyde production after 6 days illumination with fluorescent light (Castro Marín et al., 2019). The mechanism of this protection is consistent with an impact of chitosan along the Fenton-driven route of browning that involves ethanol oxidation (Fig. 1). In parallel, chitosan could also encompass the photo-Fenton pathway by inhibiting metal chelators and/or scavenging free radicals, such as HO• or 1-HER. Building on the above, it was reasoned that investigating the effect of chitosan on Fenton-unrelated 'tartaric acid' route of browning (red pathway in Fig. 1) might bring valuable information on the benefits of using this biopolymer to prevent light-induced spoilage of wines. To this end, photooxidation was induced in air saturated sulphite-free white wines and model wine solutions, and high-performance liquid chromatography with diode array detection (HPLC-DAD) was applied to evaluate the different mechanisms (shown in blue in Fig. 1) whereby browning development will be

150 affected by (*i*) various chitosan or SO_2 treatments and doses, or (*ii*) target compounds

151 acetaldehyde, glyoxylic acid, H_2O_2, iron, tartaric acid and other wine carboxylic acids, or

152 (+)-catechin.

2. Experimental

2.1. Samples, chitosan and chemicals

156 Sulphite-free, 100% Chardonnay wine samples (AOP Côteaux Champenois, vintage

157 2016) were obtained directly from the winery (Champagne J. de Telmont, Damery,

158 France). Wines were bottled in 1.5 L green glass bottles, left in darkness at 20 °C, and

159 conserved in vertical position under N_2 atmosphere after opening. The oenological

160 parameters, measured using the OIV methods of the 'Compendium of international

161 methods of analysis of wines and musts' (2018), were: ethanol, 11.35% v/v; pH 3.16;

162 titratable acidity, 4.60 g/L of sulphuric acid; volatile acidity, 0.45 g/L of sulphuric acid; malic

163 acid content < 2.0 g/L; free SO_2, < 5 mg/L, and total SO_2 < 5 mg/L.

164 Chitosan (CAS 9012-76-4; 80–90% deacetylated, average molecular weight, 10–30

165 kDa) from *Aspergillus niger*, the only source allowed for oenological purposes (OIV/OENO

166 368/2009), was obtained from KitoZyme (Herstal, Belgium). It will be termed as 'CsG' from

167 here.

168 Doubly distilled deionized water was used. HPLC grade acetonitrile and all other

169 solvents and chemicals were of the highest purity from Sigma-Aldrich (Saint Quentin

170 Fallavier, France), including the standards acetaldehyde and glyoxylic acid monohydrate,

171 (+)-catechin, (-)-epicatechin, 2,4-dinitrophenylhydrazine (DNPH), H_2O_2, ethanol, $FeSO_4$ (as

172 ferrous sulphate heptahydrate), $FeCl_3$ (as ferric chloride hexahydrate), glycine buffer, *N,N'*-

173 dimethyl-9,9'-biacridinium dinitrate (lucigenin), L-(+)-tartaric acid, L-(−)-malic acid, citric

174 acid and potassium metabisulphite.

2.2. Model wine solution

A total of 2 litres of model wine solution was prepared, containing 5 g/L (+)-tartaric acid and 12% (v/v) ethanol. After adjusting the pH to 3.2 with 5 M NaOH the solution was stirred overnight at 20 °C in open-air to reach oxygen saturation.

2.3. Preparation of solutions and suspensions for irradiation

Trials were arranged in triplicate by transferring aliquots (20 mL) of white or model wine in 50-mL high-clarity polyethylene terephthalate (PET) conical centrifuge tubes (Corning Inc., Fisher Scientific, Illkirch, France), leaving 30 mL of air in the headspace. PET has a high transmittance of about 90% within the wavelength range of 350–700 nm and is suitable for transparent applications. All samples were spiked with iron using 250 µL of freshly prepared aqueous $FeSO_4$ (1 g/L), yielding a Fe(II) concentration of 2.5 mg/L, an average value for white wines made with modern stainless-steel equipment.

Afterwards, aliquots (100 µL) of water (control samples), SO_2 (as aqueous potassium metabisulfite, to achieve 25–100 mg/L, final concentration), or weighed CsG (to achieve 0.2–2 g/L, final concentration) were added and each tube was tightly closed and dark pre-incubated at 20 °C for 48 h. The concentration levels of CsG suspensions were defined considering both the usual dosages and the maximum admitted addition in wines, equal to 1 g/L. The tubes were then irradiated for varying times (24, 48 and 240 h) by two cool daylight fluorescent lamps (Sylvania T8Luxline Plus F36 W/840) placed at a distance of 10 cm. The illumination intensity was 2000 lux (Yogokawa, 51,000 series lux meter, Lyon, France), with emission peaks centered at 313, 365, 405, 436, 546 and 578 nm, and emission peaks with maxima at 480 and 580 nm. Under these conditions no significant warming of the samples was noticed during irradiation. All samples were shaken for 2 min every hour at a 12-h period, in particular to achieve optimal contact in CsG suspensions.

Unbound acetaldehyde and glyoxylic acid levels were timely assessed throughout the entire protocol (see below).

For getting closer to the conditions of oenological usage of CsG, it was applied at 0.5–2 g/L only during dark pretreatment of iron-spiked white wine samples prepared as described above. In addition, in order to mimic real winemaking conditions, insoluble chitosan was removed by passing samples on a 0.65-µm filter before irradiation for varying times, at the end of which unbound acetaldehyde and glyoxylic acid levels in the CsG pretreated samples (termed as 'Pt-CsG') and in the related filtered controls (termed as 'Pt-controls') were measured.

In order to (*i*) examine the effect of varying iron(II) and (+)-catechin concentrations on the levels of free acetaldehyde and glyoxylic acid consequent to irradiation and (*ii*) the effect of CsG, model and white wine samples were added of iron(II) (1–5 mg/L) and (+)-catechin (0–200 mg/L), and underwent 48-h dark pretreatment followed by irradiation (for 2 or 10 days). The CsG treated group here consisted of suspensions in white wine containing 5 mg/L iron, 100 or 200 mg/L (+)-catechin, and 2 g/L CsG. Samples from each group were kept in darkness for 10 days as dark controls.

2.4.   HPLC-DAD conditions for unbound acetaldehyde and glyoxylic acid analysis

Unbound acetaldehyde and glyoxylic acid contents in samples were assayed by HPLC-DAD as their DNPH derivatives (Stocker et al., 2015). Samples (800 µL) were mixed with 200 µL of 10 mM DNPH dissolved in 2.5 M HCl, and dark incubated for 1 h at 45 ºC. After cooling at room temperature and centrifugation of the mixture (5 min at 2400g), the DNPH adducts were separated using a 250 mm × 4.6 mm i.d., 5-µm particle size Nucleodur C18 Htec column (Macherey-Nagel, Düren, Germany) with a flow rate of 0.8 mL/min. The mobile phase was a mixture of acetonitrile (solvent A) and 0.05% (v/v) phosphoric acid in deionized water (pH 2.7; solvent B) and the elution program with linear

gradient was: 0 min, 40% A, 8 min, 85% A, 9 min, 40% A, 13 min, 40% A, with an injection volume of 20 µL. A Merck Hitachi HPLC system consisting of a LaChrom L-7000 interface module and a L-7455 photodiode array detector coupled to a data processing computer (EZChrome workstation) was used. Chromatograms were acquired at 220–400 nm and derivatized compounds were identified by comparing their retention times with those of standards. Quantification was based on peak area at 360 nm from standard calibration curves.

2.5. HPLC determination of catechin and epicatechin

Separation and quantitation of catechin and epicatechin isomers were achieved at room temperature using a Htec RP-18 column (250 mm × 4 mm; 5 µm; Macherey Nagel) and a gradient with a flow rate of 0.8 mL/min. Gradient was: solvent A (0.05% H_3PO_4 in H_2O, pH 2.6), solvent B (MeOH): 0-45 min, 30–60% B; 45–50 min, 60% B; 50–51 min, 30% B; 51–57 min, 30% B. The wine samples were mixed with mobile phase (1:1 v/v) before centrifugation for 5 min at 2400g. A 20-µL volume of the supernatant was injected into the HPLC system. UV absorbance was measured at 280 nm, and quantification was carried out by comparing peak area with that of a (+)-catechin standard.

2.6. Evaluation of CsG Fe(II) and Fe(III) chelating activities

The possibility of biphasic iron(II) chelating action of CsG in wine was assessed. After 48 h dark incubation in 50-mL plastic tubes sealed with stoppers, wine samples (20 mL) saturated with air were added a mixture of 5 mg/L Fe(II) and varying concentrations of CsG (0.2–2 g/L). The resulting suspensions (termed as '+CsG') were dark incubated for an additional 48 h under continuous agitation. In another set of experiments the wine samples were first preloaded with the same concentration range of CsG and dark incubated for 48

h before 5 mg/L Fe(II) was added and the suspensions samples (termed as 'Pi-CsG') dark incubated for a further 48 h.

The iron content of the samples after filtration versus unloaded controls was then quantitated in triplicate by flame atomic absorption spectrometry according to the current official OIV method (see Castro Marín et al., 2019).

The iron(III) chelating activity of CsG was evaluated in acidified ethanolic solutions (12% v/v, pH 3.2). Samples (20 mL) loaded with 10 mg/L $FeCl_3$ were dark incubated for 1 h at 20 °C. Varying concentrations of CsG (1–10 g/L) were added thereafter under vigorous stirring. After an additional 5 min incubation the suspensions were centrifuged (2400g) for 5 min, 200 µL of each supernatant was transferred in 96-well microplates and absorbance was recorded using a microplate reader (Tecan Infinite, Männedorf, Switzerland). Experiments were made in triplicate.

2.7. Assay of H_2O_2

The amount of unreacted H_2O_2 following addition at 20 °C of CsG in H_2O_2 spiked model wine was measured by lucigenin chemiluminescence (Maskiewicz, Sogah, & Bruice, 1979). Samples (20 mL) containing H_2O_2 (100 or 500 µM) without (controls) or with added CsG (0.2–2 g/L) were placed in centrifuge plastic tubes and were dark incubated for 10 min at 20 °C. The mixture was filtered (0.45 µm nylon filter) and aliquots (20 µL) were mixed with 200 µL of a lucigenin solution (0.2 g/L in 0.2 M glycine buffer, pH 10) and dark incubated for 10 min at 20 °C in 96-well microplates before chemiluminescence was read. Blank values were measured without H_2O_2. The decrease in H_2O_2 content of CsG-treated samples was calculated as a percentage of the signal given by the corresponding control prepared as described above taken as 100%. Concentration of H_2O_2 was derived from a calibration curve (10–500 µM range) recorded in another set of lucigenin containing samples dark incubated for 10 min. Establishing the calibration curve showed that pre-

278 incubation and filtration steps in control samples resulted in a negligible loss of H_2O_2. All

279 measurements were made in triplicate.

280

281 *2.8. Browning analysis*

282 The effect of CsG and SO_2 on the susceptibility to browning was assessed in 2.5 mg/L

283 iron(II)-spiked, dark pre-incubated, then irradiated model wine solution or white wine

284 samples prepared and processed as described above for acetaldehyde and glyoxylic acid

285 measurements (see section 2.3), except that model wine samples were also added (+)-

286 catechin (100 mg/L) before dark pre-incubation. Irradiated samples were timely filtered

287 (0.45 µm nylon filter) and browning development was monitored at room temperature for

288 21 days at 420 nm by adapting the protocol of Sioumis et al. (2006) to a microplate reader.

289 Experiments were made in triplicate.

290

291 *2.9. Absorption spectroscopy of CsG-added [Fe(III)-carboxylates] complexes*

292 [Fe(III)-carboxylates] complexes were prepared in triplicate in 50-mL Falcon conical

293 centrifuge plastic tubes as previously described (Grant-Preece et al., 2017b). Briefly,

294 freshly prepared mixtures of $FeCl_3$ (20 mg/L) were stirred for 1 h at 20 °C in the dark with

295 solutions of either tartaric (5 g/L), malic or citric acids (3 g/L) in acidified ethanolic solutions

296 (12% v/v, pH 3.2). Afterwards varying concentrations of CsG (1–2 g/L) were added under

297 stirring and the mixtures were reacted in darkness a few min. Then, the mixtures were

298 centrifugated for 5 min (2400*g*), 200 µL of each supernatant was transferred into 96-well

299 microplates and the absorption was read between 256 and 496 nm at 20 °C.

300

301 *2.10. Statistical analysis*

302 Unless otherwise noted all data were analysed and presented as means ± SD for the

303 indicated number of independent experiments. Intergroup differences were calculated by

304 one-way analysis of variance (ANOVA) followed by appropriate a posteriori tests. *P*-values

305 < 0.05 were statistically significant (Prism 6 software; GraphPad Software, San Diego,

306 CA).

307

308 3 **Results and discussion**

309

310 *3.1 Development of acetaldehyde and glyoxylic acid in real and synthetic wine during*

311 *light exposure*

312 It is known that submitting iron(II)-supplemented, tartaric acid containing model

313 solutions or real white wines to fluorescent light results in an increased formation of

314 glyoxylic acid (Grant-Preece et al., 2017a, b) and acetaldehyde (Castro Marín et al., 2019),

315 the non-bounded fraction of which actively participating in wine browning phenomena.

316 Under photooxidative conditions a part of these reactive carbonyls could conceivably have

317 been formed via the established photo-Fenton mechanism (shown in green in Fig. 1)

318 through extra HO• formation and faster Fe(III)/Fe(II) recycling (Loures et al., 2013). It was

319 previously reported that chitosan, suspended in a SO_2 free Chardonnay wine added of 5.5

320 mg/L Fe(II) and allowed to chelate metal ions for 2 days in darkness, significantly inhibited

321 acetaldehyde formation upon illumination (Castro Marín et al., 2019).

322 Here a first objective was to widen these above data to photooxidation produced

323 glyoxylic acid in tartaric acid-based model matrix, and a sulphite-free white wine. After 48 h

324 of timely agitation at 20 °C in darkness with 1.5 times air volume headspace, no significant

325 acetaldehyde or glyoxylic acid formation was evidenced by HPLC-DAD in model wine

326 samples containing 2.5 mg/L iron(II) (not shown). Further lightning of these samples for 24

327 h stimulated the generation of 14.1 ± 0.7 mg/L of acetaldehyde and 108 ± 1 mg/L of

328 glyoxylic acid in the controls (Fig. 2A), consistent with the findings of Clark et al. (2007)

329 who detected glyoxylic acid only after direct sunlight exposure of model wines containing

330 tartaric acid. This production of oxidation carbonyls was directly related to illumination

time, since after 48 h the content of glyoxylic acid doubled while acetaldehyde level increased by 30% (Fig. 2A). When the experimental Chardonnay wine was stored in darkness with iron, the mean acetaldehyde concentrations of 6.1 ± 0.4 mg/L at opening remained nearly stable at 7.1 ± 0.3 mg/L after 2 days (red bar in Fig. 2B) and slightly increased up to 8.9 ± 0.3 mg/L after 10 days. At the same experimental times glyoxylic acid levels were found under the detection limits, i.e., < 2 mg/L. When storage under light exposure was applied to this wine, formation of both carbonyls was remarkably reduced with respect to model wine, especially in the case of glyoxylic acid (Fig. 2B). This could have been somewhat expected since wine macromolecules, including proteins, polysaccharides, tannins, as well as monomeric species such as phenolic acids or flavanols, may have quenched a portion of oxidizing species, particularly free radicals such as HO• (Oliveira et al., 2011), thereby decreasing the extent of ethanol or tartaric acid oxidation. After 10 days illumination, 118 ± 1 mg/L of glyoxylic acid and 18.1 ± 0.1 mg/L of acetaldehyde were measured in real wine (Fig. 2B), the latter value being close to those obtained in model solution after only 48 h (Fig. 2A).

For all the suspensions of CsG added up to 1 g/L, the level of free acetaldehyde and glyoxylic acid was dose-dependently and significantly reduced at any time of light exposure when compared to the untreated controls (Fig. 2A and B). For model wine containing 2 g/L CsG this decrease was strong for both glyoxylic acid (22.8 ± 0.2 mg/L, i.e., 79% decrease) and acetaldehyde (3.7 ± 0.7 mg/L, i.e., 77% decrease) contents after 1 day of irradiation, but illuminating the mixtures for one additional day led to a better protection for the glyoxylic acid (78% decrease) versus acetaldehyde (50% decrease) levels. A different pattern was observed in illuminated, SO_2-added model wine samples, where a stronger inhibition of both free glyoxylic acid (ranging 91–94%) and acetaldehyde (ranging 84–89%) levels was observed at 24 h and 48 h at any dose of the additive (Fig. 2A). In those samples, these reductions were considerable even at the lowest SO_2 dosage

likely due to its ability to both scavenge H_2O_2 and strongly bind aldehydes (Oliveira et al., 2011). Indeed, the apparent equilibrium constants for sulphite-aldehyde adducts were estimated to be 3.7×10^{-6} and 1.5×10^{-6} for glyoxylic acid and acetaldehyde, respectively (Sonni et al., 2011b), suggesting that a noticeable portion of those aldehydes may have been present in the bound form (Grant-Preece et al., 2017a).

Next, the progressive inhibitions of fluorescent lighting-induced build-up of acetaldehyde and glyoxylic acid seen above upon adding CsG or SO_2 were confirmed in 2.5 mg/L iron(II) added sulphite-free Chardonnay wine, again with a better effect on glyoxylic acid versus acetaldehyde levels. For example, a dose of 2 g/L CsG in suspension significantly lowered glyoxylic acid formation from 55 ± 2 mg/L to 17.6 ± 0.3 mg/L after 48 h irradiation, and such protection was even significantly better than that provided by adding SO_2 up to 100 mg/L instead of CsG (Fig. 2B). Interestingly, after 10 days of lighting the glyoxylic acid content markedly increased in all wine samples but 0.5 g/L CsG, a concentration below the maximum authorized dose for winemaking, guaranteed a significantly better control of this glyoxylic acid generation when compared to any dose of SO_2 (Fig. 2B). When wine samples were kept in contact with 1–2 g/L CsG over the 10-days irradiation time, glyoxylic acid content was decreased by up to 65% compared to controls or SO_2-treated samples. This dramatic increase might be due to an early and almost complete consumption of sulphur dioxide, e.g., by oxidation with H_2O_2 generated by thermal Fenton pathway (Fig. 1), making insufficient its potential to bind glyoxylic acid at day 10. Figure 2B also shows an opposite situation was observed for acetaldehyde levels which were significantly best inhibited by SO_2 (maximum value of 60% at day 10) than by CsG (only 23% inhibition at 2 g/L), and this acetaldehyde versus glyoxylic acid difference may be the reflection of the better binder behaviour of the former toward SO_2 (as their above cited equilibrium constants suggest).

382   Fungal chitosan at 1 g/L has been found poorly soluble in red wine (i.e., < 0.9%; Filipe-

383 Ribeiro, Cosme & Nunes, 2018) and practically insoluble in white wine after 12 h of contact

384 under gentle stirring (Colangelo et al., 2018). Therefore, its presence in bottled products

385 could be prevented by racking, membrane filtration or centrifugation (Spagna et al., 1996).

386 Recent studies have reported a good acetaldehyde control by CsG in white wine after

387 several days of light exposure following a dark pretreatment / filtration sequence (Castro

388 Marín et al., 2019). Given the positive results of Fig. 2B showing a marked inhibition of

389 glyoxylic acid formation in the unfiltered protocol after only 24 h of irradiation, it seemed

390 interesting to investigate the behaviour of CsG suspensions submitted to membrane

391 filtration before being irradiated for short times. For this purpose, the experimental 2.5

392 mg/L iron(II) spiked, non-sulphited Chardonnay wine was loaded for 48 h in darkness with

393 different doses of CsG and the suspensions passed through a 0.65-µm filter prior to 24 or

394 48 h light exposure (Pt-CsG samples).

395   After filtration the carbonyls levels of non-irradiated, unsupplemented wine samples

396 (dark controls, red bars in Fig. 2C) remained relatively low, close to that of unfiltered

397 samples (Fig. 2B). As expected, forced aeration of wine samples during filtration notably

398 increased acetaldehyde and glyoxylic acid concentrations upon irradiation in

399 unsupplemented controls (Fig. 2C) compared to unfiltered samples (Fig. 2B). All Pt-CsG

400 samples exhibited significantly lower levels of carbonyls compared to Pt-Controls, i.e., they

401 decreased by 47% for glyoxylic acid and 35% for acetaldehyde after 48 h of irradiation

402 following dark pretreatment with 2 g/L CsG. From Fig. 2B and C it was clearly seen that,

403 compared to the unsupplemented controls, pre-incubating the wine with a CsG dose as

404 low as 0.5 g/L followed by 1 day illumination resulted in a better relative inhibition of

405 glyoxylic acid formation in the filtered (–37%) than in the unfiltered (–16%) samples whilst

406 acetaldehyde development was not affected. Nevertheless, at the highest tested CsG

407 doses, the contents of both oxidation carbonyls were always best inhibited when CsG was

present in the wine during irradiation. For example, at 2 g/L CsG and after 48 h irradiation, the inhibitions in the CsG versus the Pt-CsG samples were of 34% and 21%, respectively for acetaldehyde, and 68% and 49%, respectively for glyoxylic acid. Besides confirming the enhanced trend for chitosan to slower glyoxylic acid versus acetaldehyde formation seen above, marked differences for low versus high CsG doses seem consistent with EPR data showing a biphasic interfacial antioxidant action initiated by metal chelation followed, if enough uncomplexed CsG is still available, by direct scavenging of radical species intermediates of the thermal and photo-Fenton mechanisms of Fig. 1 (Castro Marín et al., 2019). This biphasic action would therefore be relevant in the case of extended contact of chitosan with wine (e.g., during storage in tank) while in filtered and bottled wines the antioxidant activity coming from the chelating properties of CsG will probably prevail.

3.2   *Iron chelating capacity*

Direct inactivation of metal catalysts, especially Fe(II)/Fe(III) or copper, at any stage of the thermal Fenton reaction leading to acetaldehyde and glyoxylic acid (Fig. 1), is the major complementary mechanism conceivable for chitosan as an alternative or complement to SO_2 in the control of wine oxidation and reduction of browning (Bornet & Teissedre, 2008; Chinnici et al., 2014; Colangelo et al., 2018, Castro Marín et al., 2019). First, two CsG addition protocols were compared for their chelating efficiency in experimental sulfite free Chardonnay wine added 5 mg/L Fe(II). Flame atomic absorption spectrometry indicated an average content of 0.39 mg/L for total iron at opening, remaining almost stable at 0.42 mg/L after 48 h aerial dark incubation with stirring. Addition of a mixture of 5 mg/L Fe(II) + CsG (0.2–2 g/L) to the wine (+CsG samples) resulted in a dose-dependent decrease of total iron content after an additional 48 h incubation in darkness (Fig. 3A, white bars). Under the same concentration conditions a significant better iron removal was observed when the wine was added of CsG during pre-

incubation, followed by iron for the remaining 48 h incubation (Pi-CsG samples). Hence, for the same 0.5 g/L CsG input that already provided a good protection against Gly development during 24 h irradiation of the iron(II) added wine (Fig. 2C), only 24% of initial iron was removed in +CsG samples while a higher loss of about 48% was found in Pi-CsG samples (Fig. 3A, black bars). A ~40% iron reduction has been reported when a white wine naturally containing a threefold higher iron content was put in contact with 1 g/L chitosan for 12 h (Colangelo et al., 2018).

The interaction of iron with chitosan is an intricate molecular process comprising chelation, ion-exchange, and surface adsorption (Bornet & Teissedre, 2008; Gylienė, Binkienė, Baranauskas, Mordas et al., 2014) involving the lone pairs of amino groups of the polysaccharide (Fig. 1). In fact, no chitosan-complexes with, e.g., free Fe(III) can directly form at wine pH because of the preferred protonation of amino into ammonium groups and the ensuing repulsive electrostatic interactions establishing with metal cations. For this reason, ternary complexes between chitosan and anionic forms, such as [Fe(III)-tartrate] complex schematically represented in Fig. 1, may form in wine (Rocha, Ferreira, Coimbra, & Nunes, 2020).

It can be inferred from the green pathway in Fig. 1 that decreasing the catalytic activity of iron(III) in wine will participate in limiting the photoproduction of acetaldehyde. This property of CsG was demonstrated by UV-Vis spectrophotometry in a simplified solution consisting of ferric chloride (10 mg/L) dissolved in 12% v/v ethanol (pH 3.2). After 1 h dark incubation the control absorption spectrum exhibited a small shoulder at 297 nm, characteristic of $Fe(OH)^{2+}$ (Loures et al., 2013). Figure 3B shows that the whole spectrum (256–496 nm) was dose-dependently inhibited by incremental additions of CsG (1-10 g/L).

3.3 *Scavenging of H_2O_2*

Maybe the most efficient intervention to prevent photooxidation of wines is to limit or suppress the continuous formation of H_2O_2 which occurs at several steps of the thermal and photo-Fenton processes (Fig. 1). In this regard and beyond increasing consumers mistrust, sulphites are still considered essential additives for wine quality. Among other antioxidant effects (Oliveira et al., 2011), SO_2 is prone to interrupt thermal Fenton reactions by directly scavenging H_2O_2 to yield sulfate (Danilewicz, 2007, 2012; Waterhouse & Laurie, 2006). The mechanism of the reaction of H_2O_2 with chitosan in homogeneous solution has been investigated in detail (Chang, Tai, & Cheng, 2001; Qin et al., 2002) but information is scarce for what concerns its behaviour at pH and for addition modes (e.g., in suspensions) relevant to wine.

To gain insights on this matter, CsG suspensions (0.2–2 g/L) in H_2O_2 added model wine solution were stirred for 10 min at ambient temperature in darkness, and residual hydrogen peroxide was assayed by the lucigenin assay after removal of chitosan by filtration. Despite the very high H_2O_2 concentrations of 100 and 500 μM tested (see Castro Marin et al., 2019), a strong concentration-dependent inhibition was observed over a winemaking range of CsG (Fig. 3C), thus, at the maximum tested concentration of 2 g/L CsG removed 76 and 102 μM of the initial 100 and 500 μM of H_2O_2 in the samples, respectively. Based on EPR data on model wine solutions estimating that total H_2O_2 levels produced by the thermal Fenton reaction (i.e., in darkness) catalyzed by wine-like iron are within the micromolar range (Castro Marín et al., 2019), the data herein suggest that H_2O_2 scavenging may play a further antioxidant role in wine oxidation. This includes photo-Fenton conditions where accumulation of hydrogen peroxide has been demonstrated in tartaric acid containing model wine solutions (Fig. 1; Clark et al., 2007). Mechanistically, it has been proposed that peroxide scavenging by chitosan could result in its depolymerization via a metal-sensitive oxidative breakdown of the 1.4-β-glycosidic

linkages of the polysaccharide backbone, leading to decrease of apparent molecular weight of the polymer (Chang et al., 2001).

3.4 *Browning development*

Having assessed the mechanisms linked to Fenton chemistry by which chitosan, in suspension at winemaking doses, interfered with the photoproduction of acetaldehyde and glyoxylic acid, the next step of the study was to measure its anti-browning effect compared to SO_2 under the conditions of Fig. 2B. According to the mechanism of formation of (+)-catechin derived xanthylium cation pigments of Fig. 1, aerial oxidations of tartaric based model solutions containing 100 mg/L of this flavan-3-ol, and sulphite-free Chardonnay wine were initiated by adding 2.5 mg/L iron(II) during dark incubation of the samples, and optical density at 420 nm (A_{420}) was monitored in filtered samples throughout ensuing light exposure.

Figure 4A depicts the kinetics of A_{420} increase in model wine solutions. All solutions remained colorless after dark pretreatment and a lag time of 2 days was observed before brown color developed in all illuminated samples. No significant change in absorption values was seen in additional samples kept in the dark (dark controls) up to 21 days. Compared to the controls (day 0) all treated solutions had their browning development significantly decreased, with SO_2 at any dose being most effective up to day 7, before a steady increase of brown nuances appeared from day 10 up to the final recording day 21. At day 7 and onward, a significantly better dose-dependent anti-browning efficacy versus all sulphited samples was found in CsG suspensions, whose A_{420} values exhibited a plateau. After 21 days lighting, mean A_{420} values in CsG samples (combined doses) decreased by 77% and 57% compared to controls and samples added 100 mg/L SO_2, respectively. Chinnici et al. (2014) observed a lower browning tendency of model wines treated with 1 g/L chitosan, suggesting that up to 70% of the xanthylium yellow pigments

510   generated during (+)-catechin oxidation and relevant percentages of intermediate dimers

511   may adsorb onto the polysaccharide surface (see below). Consistently, the observations

512   herein on CsG solutions are probably the result of an initially faster oxidative process

513   (mediated by acetaldehyde and glyoxylic acid, and generating carboxymethine dimers and

514   brown pigments) followed by a delayed phase where the progressive accumulation of

515   dimeric intermediates and pigments is counterbalanced by their adsorption on CsG. In

516   contrast the smaller and more diffusible SO_2 will interact faster at any relevant step of the

517   browning pathways, e.g., by reducing H_2O_2, including that formed by catechin autoxidation,

518   (not represented in Fig.1 for clarity), or binding acetaldehyde and glyoxylic acid (Grant-

519   Preece et al., 2017a, b), but would stop after complete consumption of sulphites, as

520   already observed for the inhibition of 1-HER formation (Castro Marin et al., 2019).

521   Figure 4B shows the oxidative browning in experimental white wine which, at opening,

522   contained 2.9 mg/L total catechins and 1.2 mg/L total epicatechins. Right after 48 h dark

523   incubation, both SO_2 and CsG exhibited discolouring properties, having significantly

524   decreased initial absorption value up to 29% for wines incubated with 2 g/L CsG, likely by

525   an adsorption effect of phenolics on the chitosan chain and/or the lack in generation of

526   brown pigments in this latter case (Spagna et al., 1996; Chinnici et al., 2014). Again, no

527   significant change in color was seen in dark controls at day 21 versus day 0. Throughout

528   photolysis of the wines the discolouring effect of CsG was found constantly and

529   significantly higher than in SO_2 samples, with no clear dose dependency for both

530   treatments. After 21 days lighting, mean A_{420} values in CsG samples decreased by 63%

531   and 43% compared to controls and samples added 100 mg/L SO_2, respectively. It is

532   possible that this relatively poor effect of SO_2 was due to the presence in the wine of

533   quinones and carbonyls that may quench or oxidize sulphites, diminishing their anti-

534   browning efficacy. Last, it is also believed that extending the time of contact with CsG,

535   rather than increasing the dose, could had strongly improved the anti-browning effect seen

here since a recent study reported only a limited effect (as measured by OIV methods) in non-sulphited white wines stirred with 1 g/L chitosan for only 12 h (Colangelo et al., 2018). Despite catechin and epicatechin contents were found relatively low in the studied white wine (see above), it is possible that the comparable A_{420} levels shown in Fig 4B versus those of (+)-catechin added model wine (Fig. 4A) are due to the presence in the real wine of other compounds abundant in the grape juice, such as *trans*-caftaric and *trans*-coutaric acids, which, as *ortho*-diphenols, can undergo an oxidative cascade toward pigments absorbing at the same wavelength. A more obvious explanation could be related to the presence of (-)-epicatechin in the white wine, which has been consistently found to produce faster and deeper browning as compared to (+)-catechin when reacting with glyoxylic acid (Labrouche, Clark, Prenzler, & Scollary, 2005).

3.5 *Effect of catechin and CsG on photoproduction of reactive carbonyls in the presence of iron*

As schematized in Fig. 1 and suggested from the results of Fig. 4B, a complementary effect of CsG in reducing photo-assisted browning would rely on its known ability to adsorb on its surface either (+)-catechin, its colorless dimeric intermediates, or yellowish xanthylium cations (Spagna et al, 1996; Chinnici et al., 2014). The (+)-catechin model for such equivalent proanthocyanidin reactions was used to investigate the photoproduction (for two or ten days irradiation) of acetaldehyde and glyoxylic acid in model solution and (+)-catechin added Chardonnay wine dark pre-incubated (for 2 days) with varying (+)-catechin and iron concentrations.

As expected from literature data (Danilewicz, 2007), stimulating thermal and photo-Fenton oxidation routes by increasing iron concentration (1–5 mg/L) resulted in a dose-dependent increase of acetaldehyde and glyoxylic acid photoproduction (for 2 days) in all (+)-catechin free samples (Fig. 5). In real wine samples kept in darkness for 10 days (dark

controls) carbonyls remained close to background values, ranging 8 – 12 mg/L for acetaldehyde and 1– 2 mg/L for glyoxylic acid. The significant illumination-dependent increase of unbound carbonyls seen in Fig. 5 was dose-dependently reversed by incremental addition of (+)-catechin, suggesting that these oxidation products became involved in condensation reactions, leading to the formation of 8-vinyl-(+)-catechin and xanthylium cations (Fig. 1; Drinkine et al., 2005). Strikingly, this (+)-catechin dependent inhibitory effect on acetaldehyde and glyoxylic acid was almost independent from the amount of added iron, being more marked in model wine solutions. For 100 and 200 mg/L added (+)-catechin, 2 days-photoproduction for both carbonyls was inhibited by ~30% and ~50%, respectively in model solutions, and by only ~20% and ~40%, respectively in experimental wine. Extending the irradiation of the samples up to 10 days confirmed this lack of impact of iron concentration, with mean inhibitions of ~44% for glyoxylic acid and ~30% for acetaldehyde in model solutions , and only of ~20% for glyoxylic acid and ~11% for acetaldehyde in real wine, when 100 mg/L (+)-catechin was added to the samples. Actually (+)-catechin concentrations available for reacting with free acetaldehyde and glyoxylic acid in real wine were found lower than in model solutions, likely because of competition reactions for the flavanol with a variety of other wine components such as phenols or proteins (Waterhouse & Laurie, 2006). On the other hand, glyoxylic acid rather than acetaldehyde levels were found best reduced by (+)-catechin at both irradiation times (not shown at 10 days), consistent with Drinkine and co-workers (2005) who proposed a higher reactivity of (+)-catechin towards glyoxylic acid due to structural differences (e.g., functional groups and polarizability).

In order to evaluate the antioxidant contribution of CsG in inhibiting the carbonyls production seen above, it was added in suspension to the experimental wine at a dose of 2 g/L throughout the experiment. Fig. 5B shows that, in samples unsupplemented with (+)-catechin and oxidized by 5 mg/L iron(II), acetaldehyde and glyoxylic acid productions after

588   2 days photolysis decreased to concentrations similar or even lower than those obtained

589   with lower iron contents of 2 and 1 mg/L, respectively. Of the possible mechanisms

590   responsible for this early effect, metal chelation during pre-incubation could be privileged

591   (Fig. 3A), although the presence of the polysaccharide during lighting does not rule out the

592   possibility of direct radical scavenging or adsorption effects such as those implicated in

593   Fig. 4B. In connection, it was reported that putting a similar real white wine added 5.5 mg/L

594   ferrous ions in contact with 2 g/L chitosan decreased the metal content by 68% after 2

595   days in darkness (Castro Marín et al., 2019). Also, for the two (+)-catechin doses tested

596   here and for 5 mg/L added iron, inhibition by 2 g/L CsG of carbonyls photoproduction was

597   near constant in the case of glyoxylic acid (about 64%), while, for acetaldehyde, CsG

598   inhibitory efficacy was higher after the addition of 200 mg/L of the flavanol (Fig. 5B),

599   suggesting that under these conditions some adsorption of (+)-catechin onto CsG has

600   begun to occur to protect acetaldehyde levels.

601   To substantiate this hypothesis, residual (+)-catechin contents following addition of

602   100 mg/L of the flavanol ± 2 g/L CsG were determined by HPLC in those model and real

603   wine samples after irradiation for 48 h. As anticipated from Fig. 1, when added iron

604   increased from 1 to 5 mg/L, (+)-catechin consumption in untreated samples increased from

605   12.8 ± 0.7 to $24.8 \pm 1.6\%$ in model solution and from 9.8 ± 0.9 to $19.9 \pm 2\%$ in real wine.

606   When the experimental wine was oxidized by 5 m/L of iron, treatment with 2 g/L of CsG

607   significantly limited this (+)-catechin consumption to only 13% ($P < 0.05$).

608

609   3.6 *Effect of CsG on absorption spectra of tartaric, malic and citric acid wine bases in*

610   *presence of iron (III)*

611   Derived from the grapes, the α-hydroxy acids tartaric, malic and citric acids are among

612   the main contributors of wine titratable acidity (the two former being the predominant acids

613   in wine), forming stable α-carboxylate complexes with Fe(III) at wine pH. However, under

fluorescent light irradiation these ferric ion complexes decompose to acyloxyl free radicals, subsequently releasing ferrous ions to carry on the Fenton wine oxidation. Tartaric acid derived acyloxyl radicals, but not the parent species from malic and succinic acids, have been proposed (Grant-Preece et al., 2017a) as unique precursors of glyoxylic acid in the browning development, and therefore any wine additive preventing the formation of the [Fe(III)-tartrate] complex would be inhibitory (Fig. 1).

To understand if CsG fulfils this role it was reacted for a few minutes at varying concentrations with dark, pre-formed [Fe(III)-carboxylates] complexes in acidic 12% ethanolic solutions, and the mixtures were centrifugated before UV-Vis spectrophotometry was carried out. To ensure for complete reactions over the CsG concentration range used throughout, ferric ions (20 mg/L), tartaric (5 g/L), malic and citric acid (both at 3 g/L) concentrations studied here were set in large excess with respect to typical wine-like values, which are 5 mg/L, 2.7, 2.4, and 0.5 g/L, respectively. Figure 6 shows that, under these conditions, [Fe(III)-carboxylates] complexes exhibited more or less defined absorption maxima at 338 (dimer form; Danilewicz, 2014), 330, and 350 nm for tartrate (blue arrow), malate, and citrate, respectively (Grant-Preece et al., 2017b). These absorptions were distinct from that given by $Fe(OH)^{2+}$ at 297 nm (red arrow in Fig. 6; see also Fig. 3B), or by CsG alone and each individual acid. CsG (1 or 2 g/L) dose dependently reduced the optical densities near to baseline (Fig. 6), suggesting that, under the methodology used, chitosan showed strong inhibitory properties toward the tested iron complexes. However, it is not clear whether this could be related to a displacement mechanism of the carboxylates from their iron complexes since no clear UV-Vis evidence for the formation [Fe(III)-chitosan] complexes as depicted in Fig. 3B was obtained. Regarding tartrate the discovery of this property of CsG is of obvious importance since it virtually rules out the red pathway of Fig. 1 for forming glyoxylic acid-derived xanthylium cations under fluorescent lighting.

3 Conclusion

In conclusion, this work demonstrates that chitosan decreases the amount of free aldehydic intermediates related to wine photooxidation of oxygen saturated samples. In a sulphite-free Chardonnay wine inhibition as high as 80% was found for glyoxylic acid, while acetaldehyde was somewhat less affected. Particularly at doses > 0.5 g/L, the presence of chitosan significantly reduced the oxidative browning of wines to a comparable or even higher extent than did SO_2 at 100 mg/L, especially in extended oxidative conditions, because of the progressive consumption of sulphites. Notably, the antioxidant and anti-browning action of chitosan in wine samples submitted to fluorescent lighting partially persisted after its removal. Apart from aldehyde reduction, this study gained evidence that, in addition to the phenolic adsorption established in previous works (Spagna et al., 1996), these effects can be attributed to other complementary mechanisms such as iron chelation and scavenging of H_2O_2. Further, this study demonstrates for the first time the ability of chitosan to block the regeneration of Fe(II) from tartaric acid by interacting directly with the [Fe(III)-tartrate] complex intermediate.

Author contributions

A. Castro Marín and P. Stocker contributed equally to this work.

Conflict of interest

The authors declare no competing financial interest.

Figure Captions

Figure 1. General structure of chitosan and inhibitory mechanisms (blue arrows) against oxidation processes mediated by hydroxyl radical formed by (*i*) 'thermal' Fenton (pathway in black), (*ii*) photo-Fenton (pathway in green), or (*iii*) upon fluorescent lighting (pathway in red) in a sulphite-free wine. Key wine constituents and oxidation products or mediators involved in browning investigated in the study are marked in bold.

Figure 2. Effect of chitosan (CsG) or SO_2 on free acetaldehyde and glyoxylic acid formation (determined by HPLC-DAD) during fluorescent light irradiation (24–240 h) of 2.5 mg/L Fe(II)-spiked (A) model wine, and (B, C) non-sulphited Chardonnay wine. Samples were dark pre-incubated for 48 h in the absence (controls) or presence of treatments. Compounds were assayed in unfiltered samples (A, B) or in samples filtered before irradiation (C; 'Pt' samples). Red bars refer to dark pre-incubated controls maintained in darkness for: (B) 0 h, (C) 24 h (full) or 48 h (empty). One-way ANOVA followed by Duncan

test: $^+P < 0.01$ vs. corresponding dark control, $*P < 0.02$, $**P < 0.01$ and $***P < 0.001$ vs. control samples at the same time of light exposure; $^\#P < 0.01$ and $^{\#\#}P < 0.001$ vs. SO_2 (all at any doses and at the same time of light exposure). Values are means ± SD ($n = 3$–5).

Figure 3. Antioxidant properties of chitosan (CsG) related to some determinants of the thermal Fenton mechanism of wine oxidation in darkness. (A) Decrease of iron content in SO_2-free Chardonnay wine spiked with 5 mg/L Fe(II). Pi-CsG samples: wine was pre-incubated with CsG for 48 h, then iron was added and analysis occurred after 48 h additional incubation. +CsG samples: wine was incubated alone for 48 h, then CsG and iron were added simultaneously and analysis occurred after 48 h. Data are percent of the corresponding CsG free controls; (B) Absorbance spectra recorded in filtered samples 10 min after addition of CsG to 12% ethanolic solutions (pH 3.2) pre-incubated with $FeCl_3$ (10 mg/L) for 1 h. Arrow marks $Fe(OH)^{2+}$ absorption at 297 nm; (C) H_2O_2 inhibition by CsG (by lucigenin chemiluminescence) in model wine solutions spiked with H_2O_2. Percent inhibition refers to corresponding initial H_2O_2 concentrations given on top. One-way ANOVA followed by Duncan test: $**P < 0.01$ vs. CsG at the same concentration. Values are means ± SD ($n = 3$–5).

Figure 4. Development of browning (absorbance at 420 nm) during fluorescent light irradiation at 20 °C of model and non-sulphited wines spiked with 2.5 mg/L Fe(II) and effect of treatments. (A) Model wine containing 100 mg/L (+)-catechin. (B) SO_2-free Chardonnay wine. Samples were pre-incubated for 2 days in darkness and treatments were applied throughout the experiment. One-way ANOVA followed by Duncan test. $*P < 0.05$, $**P < 0.01$ and $***P < 0.001$ vs. untreated control wines at the same time of light exposure; $^\#P < 0.01$ and $^{\#\#}P < 0.001$ vs. SO_2 (all at any doses and at the same time of light

exposure); $^{§}P < 0.001$ vs. SO_2 at doses 25 and 50 mg/L. Values are means ± SD (n = 3–5).

Figure 5. Effect of varying (+)-catechin and iron(II) concentrations on photooxidation (48 h) induced free acetaldehyde and glyoxylic acid levels in (A) model wine solutions, and (B) SO_2-free Chardonnay wine. Solutions were dark pre-incubated for 48 h before illumination. Treatment with 2 g/L CsG in panel B was applied in 5 mg/L iron-spiked Chardonnay wine. One-way ANOVA followed by Duncan test: $^*P < 0.05$, $^{**}P < 0.01$ vs. (+)-catechin unsupplemented controls at the same dose of iron; $^{#}P < 0.01$ vs. iron(II) at 5 mg/L at the corresponding dose of (+)-catechin. Values are means ± SD (n = 3–5).

Figure 6. UV-Vis absorption spectra showing interaction of chitosan (CsG) with [Fe(III)-carboxylates] complexes from (A) tartaric acid (5 g/L), (B) malic acid (3 g/L), and (C) succinic acid (3 g/L). Complexes were formed in acidified 12% ethanolic solution (pH 3.2) by stirring acids with $FeCl_3$ (20 mg/L) for 1 h in darkness at 20 °C. In inhibition experiments spectra were recorded from centrifugated suspensions sampled a few min after addition of varying CsG doses to the mixtures. Arrows indicate typical maximum absorptions.

References

Barril, C., Clark, A. C., & Scollary, G. R. (2012). Chemistry of ascorbic acid and sulphur dioxide as an antioxidant system relevant to white wine. *Analytica Chimica Acta*, *732*, 186–193. https://doi.org/10.1016/j.aca.2011.11.011

Bornet, A., & Teissedre, P. L. (2008). Chitosan, chitin-glucan and chitin effects on minerals (iron, lead, cadmium) and organic (ochratoxin A) contaminants in wines. *European Food Research and Technology*, *226*, 681–689. https://doi.org/10.1007/s00217-007-0577-0

743

Bührle, F., Gohl, A., & Weber, F. (2017). Impact of xanthylium derivatives on the color of white wine. *Molecules*, *22*, 1−17. https://doi.org/10.3390/molecules22081376

746

Castro Marin, A., Culcasi, M., Cassien, M., Stocker, P., Thétiot-Laurent, S., Robillard, B., Chinnici, F., & Pietri, S. (2019). Chitosan as an antioxidant alternative to sulphites in oenology: EPR investigation of inhibitory mechanisms. *Food Chemistry*, *285*, 67–76. https://doi.org/10.1016/j.foodchem.2019.01.155

751

Chang, K. L. B., Tai, M. C., & Cheng, F. H. (2001). Kinetics and products of the degradation of chitosan by hydrogen peroxide. *Journal of Agricultural and Food Chemistry*, *49*, 4845–4851. https://doi.org/10.1021/jf001469g

755

Chinnici, F., Natali, N., & Riponi, C. (2014). Efficacy of chitosan in inhibiting the oxidation of (+)-catechin in white wine model solutions. *Journal of Agricultural and Food Chemistry*, *62*, 9868–9875. https://doi.org/10.1021/jf5025664

759

Clark, A. C., Prenzler, P. D., & Scollary, G. R. (2007). Impact of the condition of storage of tartaric acid solutions on the production and stability of glyoxylic acid. *Food Chemistry*, *102*, 905–916. https://doi.org/10.1016/j.foodchem.2006.06.029

763

Colangelo, D., Torchio, F., De Faveri, D. M., & Lambri, M. (2018). The use of chitosan as alternative to bentonite for wine fining. Effect on heat-stability, proteins, organic acids, colour, and volatile compounds in an aromatic white wine. *Food Chemistry*, *264*, 301–309. https://doi.org/10.1016/j.foodchem.2018.05.005

768

Cruz, L., Brás, N. F., Teixeira, N., Fernandes, A., Mateus, N., Ramos, M. J., Rodríguez-Borges, J., & De Freitas, V. (2009). Synthesis and structural characterization of two diastereoisomers of vinylcatechin dimers. *Journal of Agricultural and Food Chemistry*, *57*, 10341–10348. https://doi.org/10.1021/jf901608n

773

Danilewicz, J. C. (2007). Interaction of sulfur dioxide, polyphenols, and oxygen in a wine-model system: Central role of iron and copper. *American Journal of Enology and Viticulture*, *58*, 53–60.

Danilewicz, J. C. (2012) Review of oxidative processes in wine and value of reduction potentials in enology. *American Journal of Enology and Viticulture*, *63*, 1-10.

Danilewicz, J. C. (2014). Role of tartaric and malic acids in wine oxidation. *Journal of Agricultural and Food Chemistry*, *62*, 5149–5155. https://doi.org/10.1021/jf5007402

Drinkine, J., Glories, Y., & Saucier, C. (2005). (+)-Catechin−aldehyde condensations: Competition between acetaldehyde and glyoxylic acid. *Journal of Agricultural and Food Chemistry*, *53*, 7552–7558. https://doi.org/10.1021/jf0504723

Elias, R. J., Andersen, M. L., Skibsted, L. H., & Waterhouse, A. L. (2009). Identification of free radical intermediates in oxidized wine using Electron Paramagnetic Resonance spin trapping. *Journal of Agricultural and Food Chemistry*, *57*, 4359–4365. https://doi.org/10.1021/jf8035484

Es-Safı, N. E., Le Guernevé, C., Fulcrand, H., Cheynier, V., & Moutounet, M. (1999). New polyphenolic compounds with xanthylium skeletons formed through reaction between (+)-catechin and glyoxylic acid. *Journal of Agricultural and Food Chemistry*, 47, 5211–5217. https://doi.org/10.1021/jf990424g

Fulcrand, H., Dueñas, M., Salas, E., & Cheynier, V. (2006). Phenolic reactions during winemaking and aging. *American Journal of Enology and Viticulture*, *57*, 289−297.

Filipe-Ribeiro, L., Cosme, F., & Nunes, F. M. (2018). Data on changes in red wine phenolic compounds after treatment of red wines with chitosans with different structures: *Data in Brief*, *17*, 1201–1217.

Grant-Preece, P., Schmidtke, L. M., Barril, C., & Clark, A. C. (2017a). Photoproduction of glyoxylic acid in model wine: Impact of sulfur dioxide, caffeic acid, pH and temperature. *Food Chemistry*, *215*, 292–300. https://doi.org/10.1016/j.foodchem.2016.07.131

Grant-Preece, P., Barril, C., Schmidtke, L. M., & Clark, A. C. (2017b). Impact of fluorescence lightning on the browning potential of model wine solutions containing organic acids and iron. *Journal of Agricultural and Food Chemistry, 65*, 2383−2393. https://doi.org/10.1021/acs.jafc.6b04669

Gyliené, O., Binkiené, R., Baranauskas, M., Mordas, G., Plauškaité, K., & Ulevičius, V. (2014). Influence of dissolved oxygen on Fe(II) and Fe(III) sorption onto chitosan. *Colloids and Surfaces A : Physicochemical and Engineering Aspects*, *461*, 151–157. https://doi.org/10.1016/j.colsurfa.2014.07.027

Labrouche, F., Clark, A. S., Prenzler, P. D., & Scollary, G. R. (2005). Isomeric influence on the oxidative coloration of phenolic compounds in a model white wine: Comparison of (+)-catechin and (-)-epicatechin. *Journal of Agricultural and Food Chemistry*, *53*, 9993−9998. https://doi.org/10.1021/jf0511648

Loures, C. C. A., Alcântara, M. A. K., Filho, H. J. I., Teixeira, A. C. S. C., Silva, F. T., Paiva, T. C. B., & Samanamud, G. R. L. (2013). Advanced oxidative degradation processes: fundamentals and applications. *International Review of Chemical Engineering*, *5*, 102−120.

Marchante, L., Marquez, K., Contreras, D., Izquierdo-Cañas, P. M. García-Romero, E., & Días-Maroto, M. C. (2020). Potential of different antioxidant substances to inhibit the 1-hydroxyethyl radical in SO_2-free wines. *Journal of Agricultural and Food Chemistry*, *68*, 1707−1713. https://doi.org/10.1021/acs.jafc.9b07024

Maskiewicz, R., Sogah, D., & Bruice, T. C. (1979). Chemiluminescent reactions of lucigenin. 1. Reactions of lucigenin with hydrogen peroxide. *Journal of the American Chemical Society*, *101*, 5347−5354. https://doi.org/10.1021/ja00512a040

Mateus, N. Silva, A. M. S., Santos-Buelga, C., Rivas-Gonzalo, J. C., & De Freitas, V. (2002). Identification of anthocyanin-flavanol pigments in red wines by NMR and mass spectrometry. *Journal of Agricultural and Food Chemistry*, *50*, 2110–2116. https://doi.org/10.1021/jf0111561

Muxika, A., Etxabide, A., Uranga, J., Guerrero, P., & de la Caba, K. (2017). Chitosan as a bioactive polymer: Processing, properties and applications. *International Journal of Biological Macromolecules*, *105*, 1358–1368. https://doi.org/10.1016/j.ijbiomac.2017.07.087

Oliveira, C. M., Ferreira, A. C. S., De Freitas, V., & Silva, A. M. S. (2011). Oxidation mechanisms occurring in wines. *Food Research International*, *44*, 1115–1126. https://doi.org/10.1016/j.foodres.2011.03.050

Picariello, L., Rinaldi, A., Blaiotta, G., Moio, L., Pirozzi, P., & Gambuti, A. (2020). Effectiveness of chitosan as an alternative to sulfites in red wine production. *European Food Research and Technology, 246*, 1795–1804. https://doi.org/10.1007/s00217-020-03533-9

Qin, C. Q., Du, Y. M., & Xiao, L. (2002). Effect of hydrogen peroxide treatment on the molecular weight and structure of chitosan. *Polymer Degradation and Stability*, 76, 211–218. https://doi.org/10.1016/S0141-3910(02)00016-2

Rocha, M. A. M., Ferreira, P., Coimbra, M. A., & Nunes, C. (2020) Mechanism of iron ions sorption by chitosan-genipin films in acidic media. *Carbohydrate Polymers*, 236, 116026. https://doi.org/10.1016/j.carbpol.2020.116026

Sioumis, N.; Kallithraka, S.; Makris, D. P.; Kefalas, P. (2006). Kinetics of browning onset in white wines: influence of principal redox-active polyphenols and impact on the reducing capacity. *Food Chemistry,* 94, 98–104. https://doi.org/10.1016/j.foodchem.2004.10.059

869   Sonni, F.; Clark, A. C., Prenzler, P. D.; Riponi, C.; Scollary, G. R. (2011a). Antioxidant
870   action of glutathione and the ascorbic acid/glutathione pair in a model white wine. *Journal*
871   *of Agricultural and Food Chemistry*, *59*, 3940–3949. https://doi.org/10.1021/jf104575w

872

873   Sonni, F., Moore, E. G., Clark, A. C., Chinnici, F., Riponi, C. & Scollary, G. R. (2011b).
874   Impact of glutathione on the formation of methylmethine- and carboxymethine-bridged (+)-
875   catechin dimers in a model wine system. *Journal of Agricultural and Food Chemistry*, *59*:
876   7410–7418. https://doi.org/10.1021/jf200968x

877

878   Spagna, G., Pifferi, P. G., Rangoni, C., Mattivi, F., Nicolini, G., & Palmonari, R. (1996).
879   The stabilization of white wines by adsorption of phenolic compounds on chitin and
880   chitosan. *Food Research International*, *29*, 241–248. https://doi.org/10.1016/0963-
881   9969(96)00025-7

882

883   Stocker, P., Ricquebourg, E., Vidal, N., Villard, C., Lafitte, D., Sellami, L., Pietri, S.
884   (2015) Fluorimetric screening assay for protein carbonyl evaluation in biological samples.
885   *Analytical Biochemistry*, *482*, 55–61. https://doi.org/10.1016/j.ab.2015.04.021

886

887   Vally, H., Misso, N. L. A., & Madan, V. (2009). Clinical effects of sulphite additives.
888   *Clinical & Experimental Allergy*, *39*, 1643–1651. https://doi.org/10.1111/j.1365-
889   2222.2009.03362.x

890

891   Waterhouse, A. L., & Laurie, V. F. (2006). Oxidation of wine phenolics: A critical
892   evaluation and hypotheses. *American Journal of Enology and Viticulture*, *57*, 306–313.

Figure 1
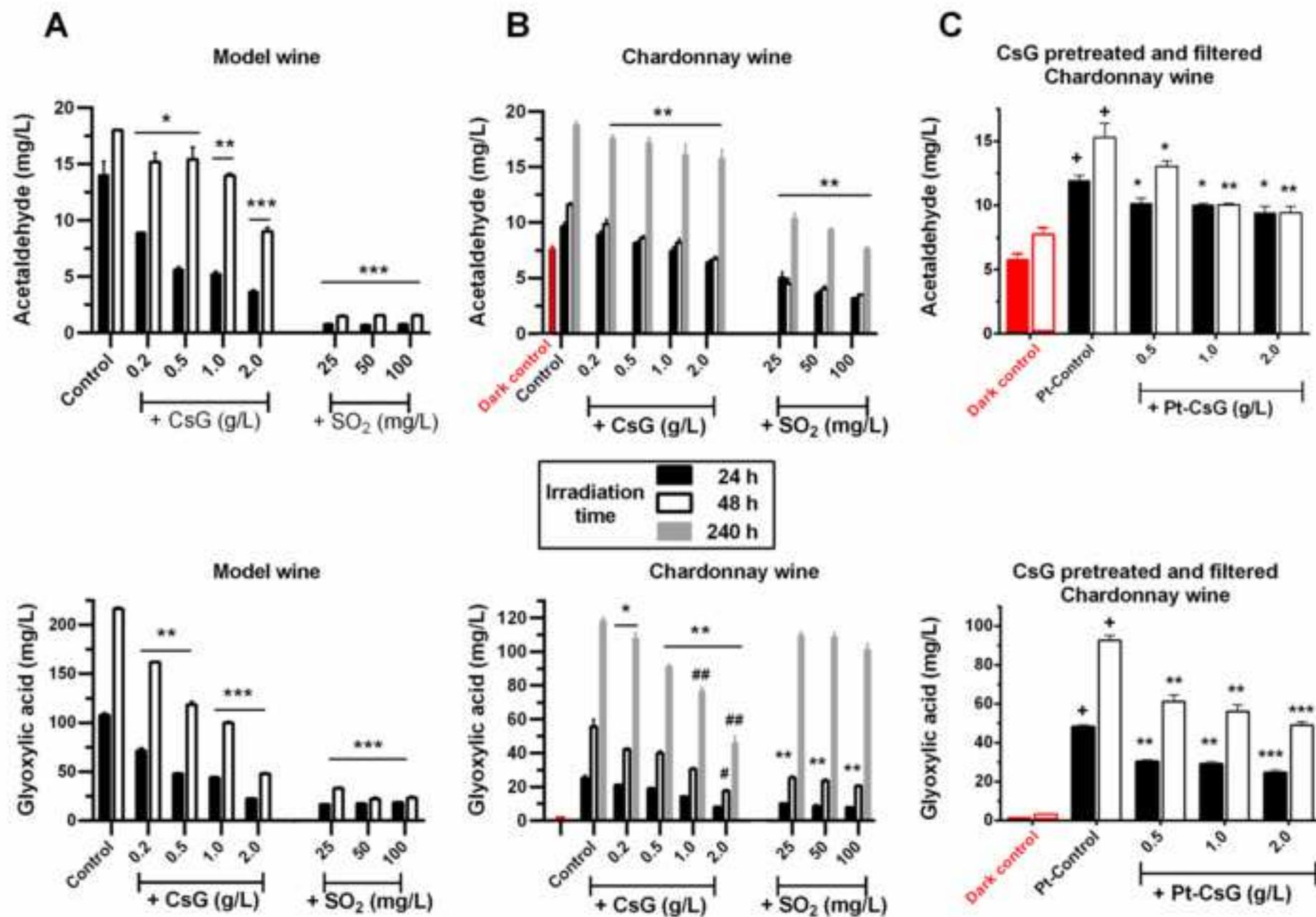**Click here to download high resolution image**

Figure 1

Figure 2
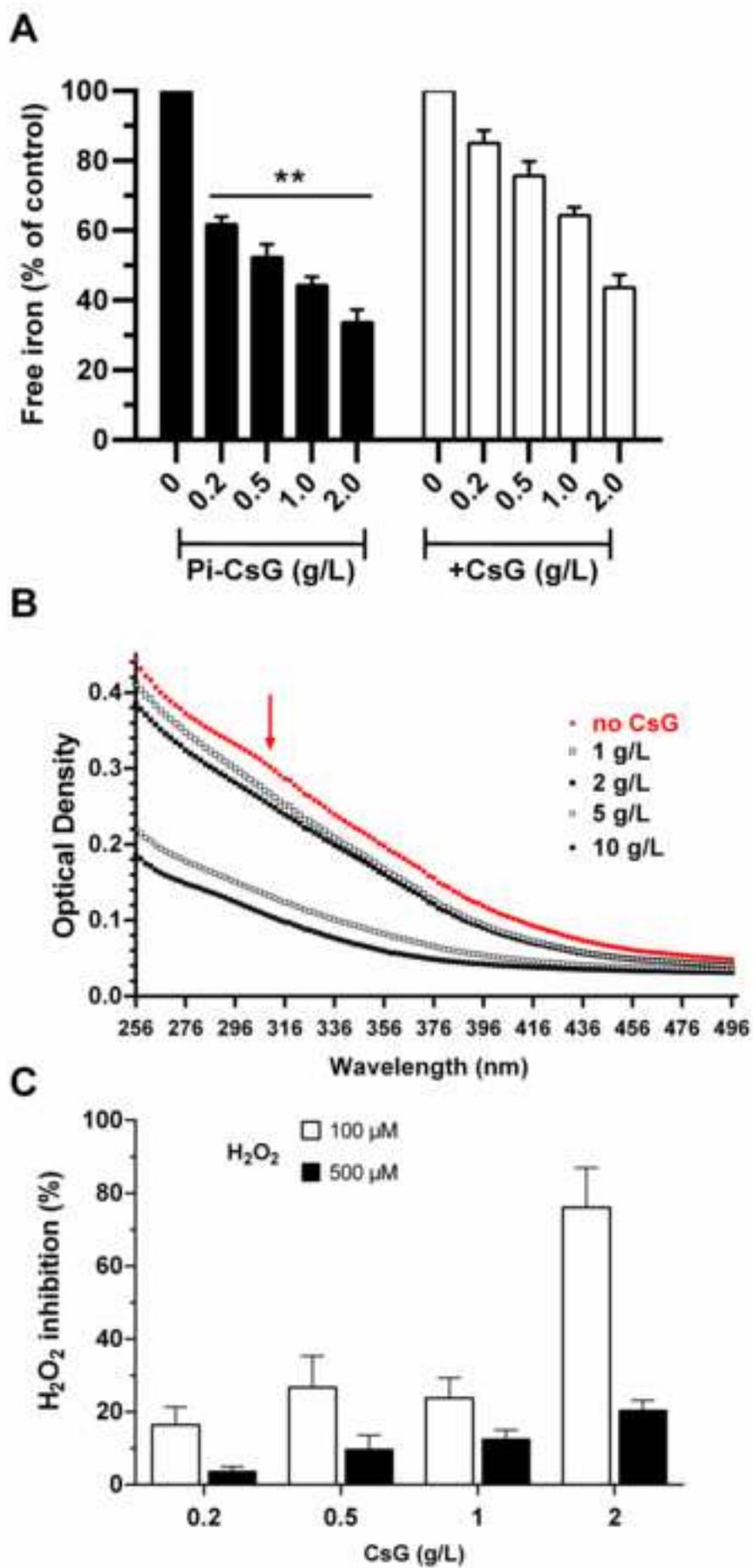**Click here to download high resolution image**

Figure 3

Figure 4
Click here to download high resolution image
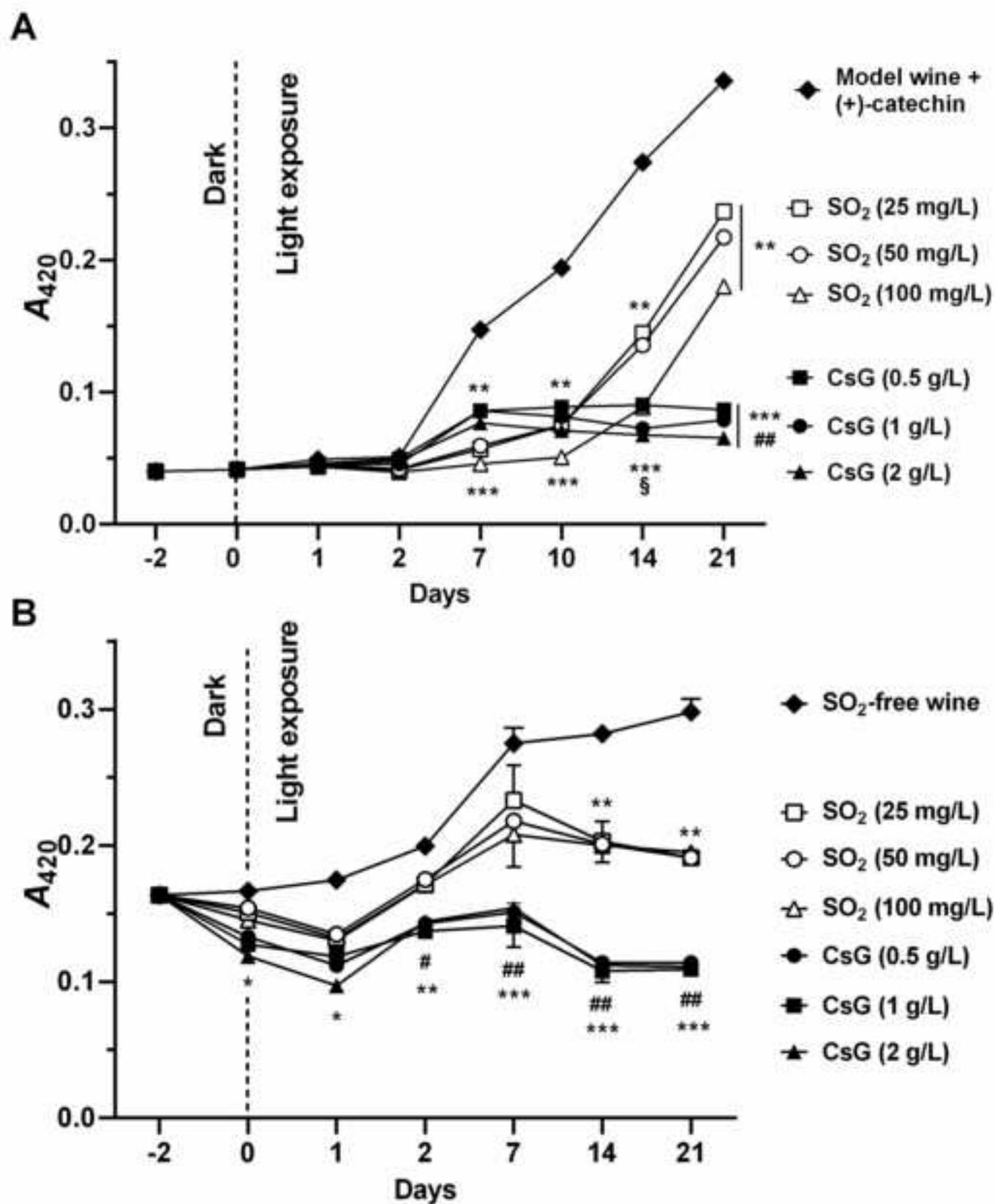
Figure 5
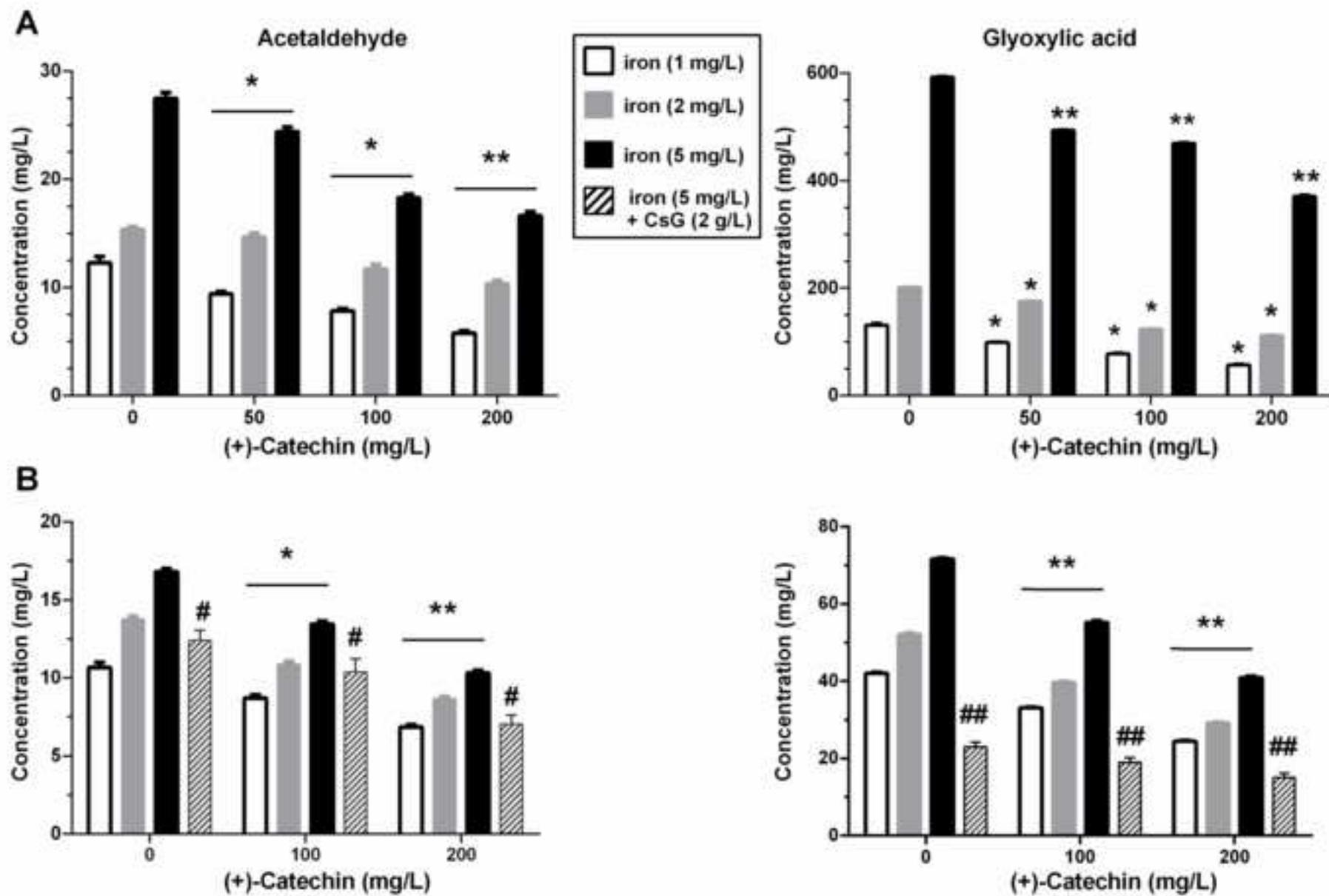**Click here to download high resolution image**
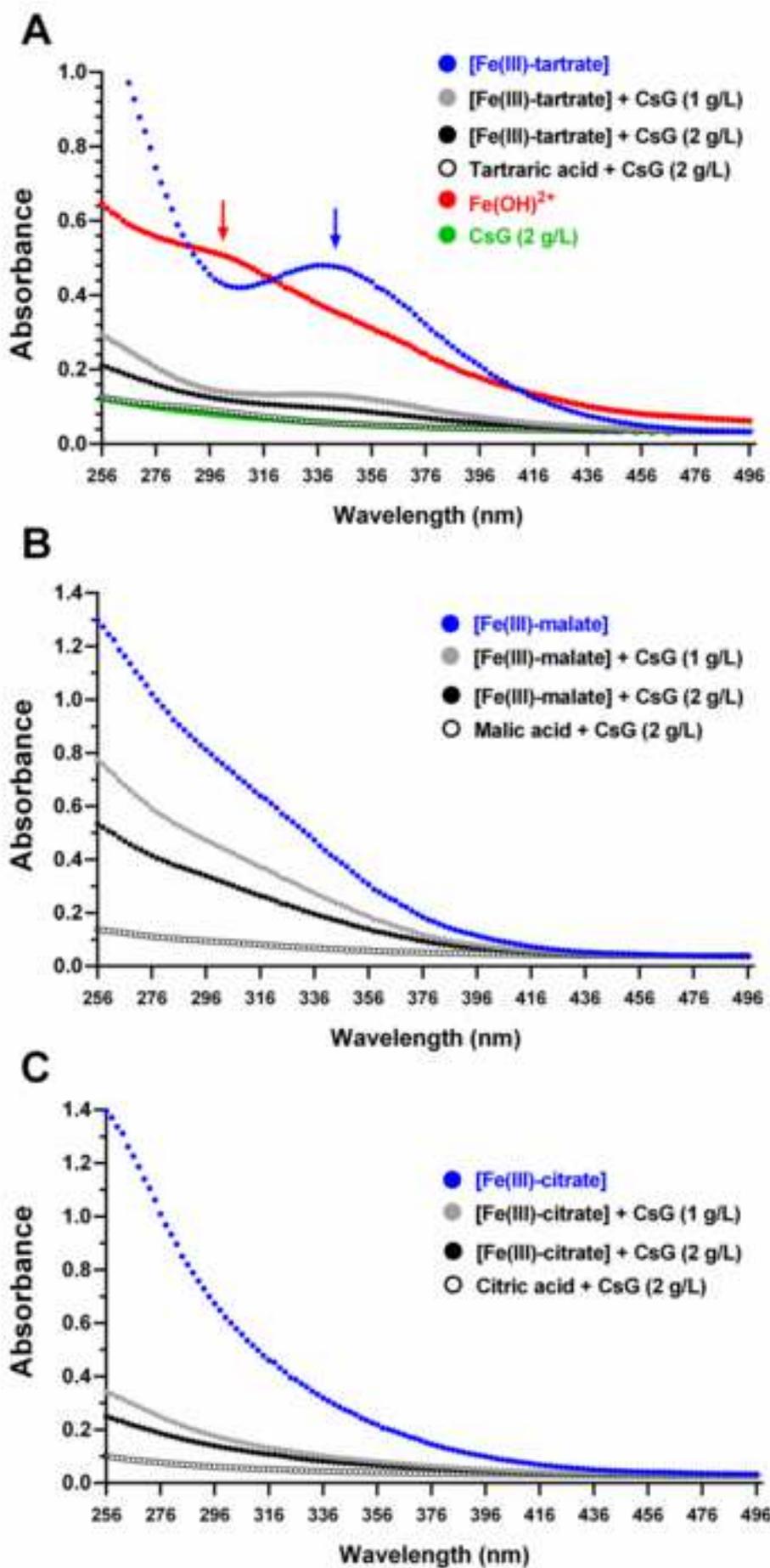

Figure 5

Figure 6
Click here to download high resolution image

1. Fungoid chitosan reduces the generation of aldehydes during wine photo-oxidation

2. Chitosan reduces iron amounts in solution by adsorbing [carboxylates-Fe(III)] complexes

3. In extended oxidative conditions SO_2 is a poorer wine anti-browning agent than chitosan

4. Sulphites better control free acetaldehyde but not glyoxylic acid amounts

5. In wines chitosan can mitigate the browning while preserving catechin amounts

Declaration of interests

☒ The authors declare that they have no known competing financial interests or personal relationships that could have appeared to influence the work reported in this paper.

☐The authors declare the following financial interests/personal relationships which may be considered as potential competing interests: